

PACS numbers: 62.20.Qp, 68.37.Hk, 68.55.jd, 81.15.Rs, 81.20.Wk, 81.40.Pq, 81.65.Ps

## Improving Wear Resistance for Grinding Balls of Horizontal Cement Mill in Cement Plant by Nanocoating Technique

Ali Sadiq Alithari and Oday Khadem Mohammed

*University of Kufa, Faculty of Engineering,  
Mechanical Engineering Department,  
540011 Kufa, Najaf Governorate, Iraq*

The grinding media play an important role in cement industry, and these balls suffered from severe wear during the grinding process of clinker. The aim of this investigation is to decrease the wear rate of the grinding balls used in horizontal cement mills by using nanocoating of tungsten carbides WC. The samples of white cast iron are prepared according to standards of ASTM 522 and DIN 1669 German for microhardness test and wear test (pin on disc). High-velocity oxy-fuel system used to coat the samples with a thickness of 50, 70, and 80  $\mu\text{m}$  with nanoparticles of WC. The results show that the best coat thickness is of 70  $\mu\text{m}$  that gives good results and best adhesion with the base material. The presence of nanocoating on sample surface increases the wear resistance by about 75% and increases the microhardness by about 14.6% for samples coated with 70  $\mu\text{m}$  layer thickness.

Шліфувальні середовища відіграють важливу роль у цементній промисловості, та ці деталі зі сферичною поверхнею «страждали» від сильного зносу в процесі шліфування клінкеру. Метою цього дослідження є пониження швидкості зносу шліфувальних кульок, що використовуються в горизонтальних цементних млинах, за допомогою нанопокриття з карбідів вольфраму WC. Зразки білого чавуну готуються за стандартами ASTM 522 і DIN 1669 (Німеччина) для тестування на мікротвердість і знос (шпилька на диску). Високошвидкісна газополуменева система використовується для покриття зразків товщиною 50, 70 і 80 мкм наночастинками WC. Результати показують, що найліпша товщина покриття становить 70 мкм, що дає хороші результати та найліпше зчеплення з базовим матеріалом. Наявність нанопокриття на поверхні зразка збільшує зносостійкість приблизно на 75% і збільшує мікротвердість приблизно на 14,6% для зразків, покритих товщиною шару у 70 мкм.

**Key words:** high-chromium white cast irons, tungsten carbide (WC) nanoparticles, HVOF system, wear test, microhardness test.

**Ключові слова:** високохромисті білі чавуни, наночастинки карбиду вольфраму (WC), високошвидкісна газополуменева система, тест на знос, тест на мікротвердість.

(Received 27 August, 2020)

## 1. INTRODUCTION

Cement grinding process takes place in horizontal mill that contains from two-compartment, the first part with coarse grinding compartment provided with a step lining that is suitable for large grinding media and ensures optimum lifting of the mill charge. The balls charge mill consists of grinding media with various sizes to ensuring optimum grinding efficiency and easy maintenance. For fine grinding, the charge consists of small balls, which ensures the best possible grinding efficiency without obstructing the material flow through the balls charge, these metallic balls are subjected to wear and failure due to its movement and collisions inside the mill [1].

Xinghai Shao *et al.* studied the effects of using TiN nanoparticles on the high-chromium white cast iron. Performance of microanalysis and wear-resistant studied. The wear resistance improved up to 59% after the addition amount of TiN is 2% [2].

Bhattacharjee *et al.* investigated the wear performance of the dry sliding of WC reinforced cast iron matrix composites carried out at 25°C. Three sets of specimens consist of powder of cast iron (of 3% wt.) and size range from 5 to 15  $\mu\text{m}$ . The WC reinforced cast iron (of 3% wt.) and nanosize of 35 nm of synthesis using WC airpower technology method for check the wear and friction performance at different forces. Results show increasing in microhardness of the degree by 2.5 times as investigated in the case of 3% wt. The wear rate a range was from 1.37 to 1.46 times lower than in the case of nanocomposites compared to the unreinforced iron specimens [3].

Higuera-Cobos *et al.* studied the influence of nanoparticles of WC on the microstructure of the hard surface of (cast-iron) by SEM and XRD devices. The friction and wear performance of the hard facing alloys with different nanoparticles noticed using the pin on disc sliding test of wear. The results indicated that the volume fraction of  $\text{M}_7\text{C}_3$  in the hard facing alloy with 0.278% wt. nanoparticles increased by 26% than that of the hard surface alloy without nanoparticles. The microhardness of the hard surface of specimens' nanoparticles was of 710 *HV*. The hardness of the hard facing alloy with 0.278% wt. nanoparticles reached to 720 *HV*. The wear rate of the hard facing alloy with 0.278% wt. nanoparticles was decreased by 20% than the hard facing alloy without nanoparticles [4].

Santos *et al.* studied the effects of tungsten carbide (WC) nanoparticles on mechanical properties of the AISI 1020 standardized steel. The heat treatment process done by tempered and quenched with a WC nanoparticles' coating. Abrasive wear and micro hardness tests are done according to the ASTM (G99-17) specification. The results shows that the micro hardness of the AISI 1020 increased by 5.4%. The abrasive wear resistance increase by 122% compared with uncoated specimens [5]. This investigation tries to find a technique to improving the wear resistance of metallic grinding balls.

## **2. GRINDING BALL**

The mill rotation causes the charge that consisting of grinding ball and feed material to be lifted over some distance by friction between the media and the lining. In Figure 1, grinding media is shown inside mill. The height to which the charge lifted depends on certain factors [6]: 1) rotating speed of the mill; 2) weight, size, and shapes of grinding ball; 3) the friction force between the mill lining and the grinding ball; 4) internal friction mill charge.

## **3. THE MATERIAL USED**

### **3.1. High-Chromium White Cast Iron (HCWCI)**

In the form of castings, heat-treated alloy is used to improved wear resistance and equipment longevity [7]. High-chromium white cast iron used in (impellers and casing, piping components, parts exposed to high wear such as bends, elbows, reducers, breaker screens, wear liners, nozzle inserts, and cyclones). Table 1 shows the chemical composition of high-chromium white cast iron.

### **3.2. Tungsten Carbide (WC) Nanoparticles**

The nanoparticles of tungsten carbides have the physical properties as follow: black hexagonal crystals; melting point  $2870^{\circ}\text{C} \pm 50^{\circ}\text{C}$ ; boiling point  $6000^{\circ}\text{C}$ ; dissolved in mixed acid of nitric acid and hydrofluoric acid, also in the aqua region; insoluble in cold water; the relative density of 15.63; strong acid resistance; high hardness; high elastic modulus [8]. The tungsten carbides may be used for production of various alloys, producing high ability nanocrystalline or superfine horniness alloy, hard-face abrasion-resistant spraying and petrochemical cracking catalyst; chip less forming tools; cutting tools; mining tolls; wear-resistance coatings; corrosion-

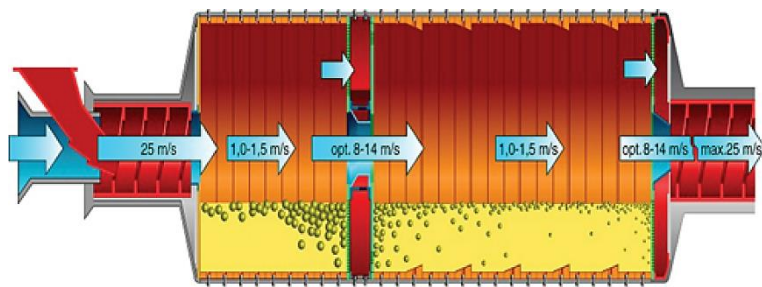


Fig. 1. Microhardness with coating thickness.

TABLE 1. Chemical composition high-chromium white cast iron.

Element	C, %	Si, %	Mn, %	P, %	S, %	Cr, %	Mo, %	Ni, %	Al, %	Co, %	Cu, %	Fe, %
HCCI	2.3	0.867	0.67	0.03	0.04	17	0.1	0.194	0.03	0.18	0.15	Bal.

resistant coatings; wear-resistant parts [9].

#### 4. EXPERIMENTAL WORK

The materials used in the production of the surface layer using a thermal coating technique by flame spraying technology. The equipment used in the coating process and the practical method used in coating samples of high-chromium white cast iron There are three axes of practicality manufacturing models manufacturing thermal coating system and examination of models.

##### 4.1. Assembly the Thermal Coating System (HVOF) and Coating Method

The High-Velocity Oxy-Fuel (HVOF) system assembled in the Laboratory of Applied Mechanics and the Nanotechnology, Department of Mechanical Engineering at Kufa University, Iraq. The coating was done for the samples after the operation of the system. The oxygen ratio to the acetylene was 2:1, and the flow rate of nanoparticle and the distance between the samples was of 10 cm. Figure 2 shows HVOF system [10].

##### 4.2. HVOF Thermal Spray Technology

High-Velocity Oxy-Fuel (HVOF) thermal spray technologies allow



Fig. 2. HVOF system.

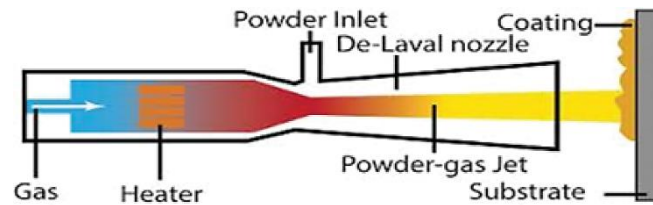


Fig. 3. Process of coating with HVOF technique.

applying coatings with extremely low porosity and high bond strength. A mixture of fuel and oxygen is combusted within a thermal spray gun producing temperatures near 6000 F (3300°C). Powder particles are injected into the high-pressure gas stream created by the combustion and accelerated down the barrel of the spray gun at several times the speed of sound. At these speeds and temperature conditions, semi-molten particles adhere to the substrate with superior bond strength exceeding 69 MPa (10,000 psi) [11]. During coating application, the product rotates methodically in front of the HVOF thermal spray gun until the coating builds to the specified thickness of 50, 70, and 80  $\mu\text{m}$ . This process creates the strongest bond and highest hardness value as compared to any other thermal spray process. Figure 3 shows the process of a coating by HVOF system.

## 5. PREPARING OF WEAR TEST (PIN ON DISC) SAMPLES

The samples of wear are preparing according to ASTM (G99-17) [12], with dimensions according to the dimensions set in standard specification, shown in Fig. 4 for disc samples. The material of pin samples made from white cast iron (Gx-26-Cr 27) by Silvana Turkish Company. The chemical compositions of pin materials tested in



**Fig. 4.** Samples of discs.



**Fig. 5.** Samples of pins.

AL-Karama General Company in Baghdad as indicated, shown in Fig. 5 with steps: 1—lathing of the samples to reach the required dimensions according to ASTM G99-04; 2—the surface of the sample smoothed to make the smoothness required for coating and testing at the Faculty of Engineering, University of Kufa; 3—cleaning the samples by emery paper made of silicon carbide with a thickness of P120; 4—place the samples at a suitable distance of 150 mm from the nozzle; 5—install the samples on the surface of the thermal bricks; 6—operation of the discharge system and introduction of Ar gas into the spray chamber; 7—operating the flame system with oxygen and acetylene ratios 2:1 to heat the samples to 800°C; 8—spray the nanoparticles of tungsten carbide with three different times: 5, 10, and 15 seconds to get coat thickness of 50, 70, and 80  $\mu\text{m}$ , respectively; 9—heat treatment where the samples heated to 1100°C and with 60 minutes' fixation time to make sure adhesion and homogeneity of the coated layer indicating the spray coating rules.

## 6. WEAR TEST (STANDARD TEST)

Wear is defined as the process of removal of material from one or both of two solid surfaces in solid-state contact. As the wear is a surface removal phenomenon and mostly occurred at outer surfaces, it is more appropriate and economical to make a surface modified of existing alloys than using the wear-resistant alloys. The pin was held against the counter face of a rotating disc made from white cast iron (GX-260 Cr 17) according to ASTM G99-17. The disc diameter is of 50 mm with 10 mm high. Figure 6 shows disc samples coating, and Fig. 7 shows disc samples divas test.

The specimen was weighed after the test, the weight difference was calculated ( $w_1 - w_2$ ), and then, the wear rate is calculated using the relation

$$\text{Wear rate} = d_w / S_d \quad [\text{g} \cdot \text{cm}^{-1}], \quad (1)$$

where  $d_w$ —the weight difference [g]:

$$\Delta w = w_1 - w_2. \quad (2)$$

The sliding distance [mm] is calculated using the relation:

$$S_d = 2\pi rn. \quad (3)$$

## 7. RESULTS AND DISCUSSION

### 7.1. Wear Test

This test carried out according to ASTM G99-17 for 12 samples



Fig. 6. Disc samples' coating.



Fig. 7. Wear test device.

without coating as indicated in Table 2 and Fig. 8 with angular speed of 400 and 600 r.p.m. and a load of 20, 40, and 60 N with test time of 10 min. The samples weighed before and after tests; the weight loss was calculated. The best of average weight loss percentage in samples without coating is 0.003798% at 400 r.p.m. by 20 N, while the average best weight loss ratio in samples with coating thickness of 70  $\mu\text{m}$  is 0.0020855% at 400 r.p.m. by 20 N.

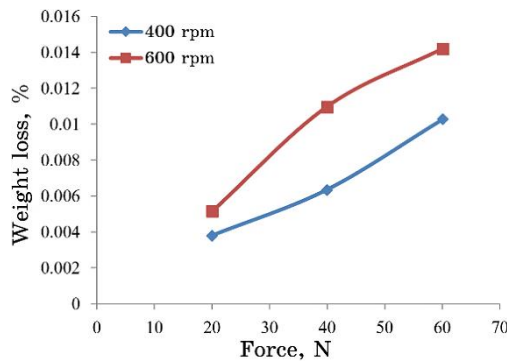


Fig. 8. Force and weight loss ratio for specimens without coating.

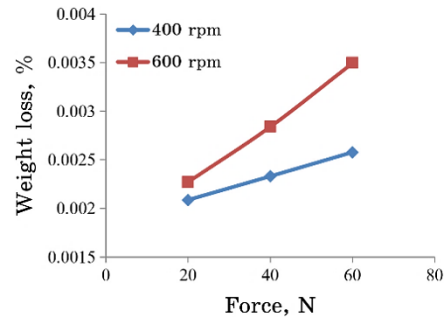


Fig. 9. Force-weight loss relation for specimens of 70  $\mu\text{m}$  coat thickness.

TABLE 2. Wear test without coating.

Sample No.	$N$ , r.p.m.	Force, N	Initial weight before wear, g	Final weight after wear, g	Weight loss	Weight loss ratio, %
1	400	20	72.2023	72.1995	0.0028	0.003877993
2		20	72.6177	72.615	0.0027	0.003718102
3		40	73.2857	73.2811	0.0046	0.006276804
4		40	73.0966	73.0919	0.0047	0.006429848
5		60	74.902	74.8945	0.0075	0.010013084
6		60	73.4588	73.4511	0.0077	0.010482066
7	600	20	72.965	72.9612	0.0038	0.005207976
8		20	72.75	72.7463	0.0037	0.005085911
9		40	74.2221	74.2139	0.0082	0.011047922
10		40	73.2999	73.2919	0.008	0.010914067
11		60	74.0624	74.0522	0.0102	0.01377217
12		60	73.903	73.8922	0.0108	0.01461375

Figure 9 presents force–weight loss relation for specimens with 70 μm coating thickness and this improvement in wear resistance due to the nanocoating layer that gave more strengthening for the surface. The coating thicknesses of 50 and 80 μm neglected because the weak thickness for 50 μm and there is an ablation and flaking for coating layer of 80 μm with low adhesion with base material.

Table 3 shows the results of wear test for samples with coat thickness of 70 μm at different angular velocities (400, 600 r.p.m.) and loads (20, 40, and 60 N) with test time of 10 min, the best im-

**TABLE 3.** Wear test for samples of 70 μm coating thickness.

Sample No.	N, r.p.m.	Force, N	Initial weight before coat, g	Initial weight after coat, g	Final weight after wear, g	Weight loss, g	Weight loss ratio%
1	400	20	73.526	73.5285	73.5269	0.0016	0.002176
2		20	75.183	75.1855	75.184	0.0015	0.0019951
3		40	76.234	76.2366	76.2348	0.0018	0.0023611
4		40	73.989	73.9915	73.9898	0.0017	0.0022976
5		60	76.1877	76.1902	76.1883	0.0019	0.0024938
6		60	75.1814	75.1835	75.1815	0.002	0.0026602
7	600	20	73.526	73.5284	73.5267	0.0017	0.002312
8		20	76.3002	76.3025	76.3008	0.0017	0.002228
9		40	73.5112	73.5137	73.5117	0.002	0.0027206
10		40	74.4006	74.4031	74.4009	0.0022	0.0029569
11		60	75.4218	75.4238	75.4211	0.0027	0.0035798
12		60	76.2344	76.237	76.2344	0.0026	0.0034104

**TABLE 4.** Wear test result (weight loss).

Force, N	Without coating		With coating (50 μm)		With coating (70 μm)		With coating (80 μm)	
	400 r.p.m.	600 r.p.m.	400 r.p.m.	400 r.p.m.	400 r.p.m.	600 r.p.m.	400 r.p.m.	600 r.p.m.
20	0.00275	0.00375	0.00155	0.0017	0.00127	0.00147	0.00115	0.00127
40	0.00365	0.00595	0.00175	0.0021	0.0016	0.00177	0.0013	0.0014
60	0.00465	0.0081	0.00195	0.00265	0.0018	0.00205	0.00157	0.00165

provement in wear resistance reach to 76% for coated sample with 70  $\mu\text{m}$ , as show the coating layer gave more stiffness for metal surface and made it more strength for external effects.

Table 4 shows the wear rate for different coat thickness samples at different load and different angular velocity, and can notice the improvement in wear resistance when increasing the coat thickness and largest value of improvement for sample with coat thickness of 70  $\mu\text{m}$ , as the nanocoating gives more resistance for surface to penetrating and removal of materials from surface.

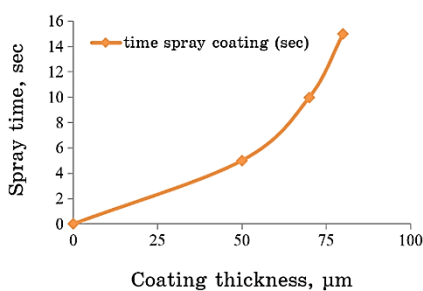


**Fig. 10.** Relationship between spray time and coating thickness.

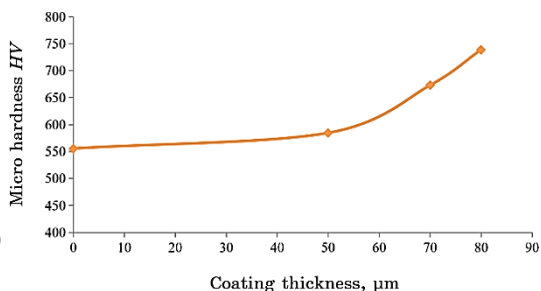


**Fig. 11.** Microhardness with coating thickness.

**TABLE 5.** Microhardness *HV*.

Number	<i>HV</i> hardness without coating	<i>HV</i> hardness coating thickness (50 $\mu\text{m}$ )	<i>HV</i> hardness for coating thickness (70 $\mu\text{m}$ )	<i>HV</i> hardness for coating thickness (80 $\mu\text{m}$ )
1	554.9	600.3	669.1	740.2
2	556.4	585.2	671.4	742.1
3	555.8	595.4	670.9	737.2
4	556.4	580.7	674.1	733.4
5	554.9	579.4	671.6	734.8
6	556.1	582.1	678.2	742.2
7	554.7	577.4	674.6	743.7
8	557	578.2	676.8	740.8
Average	555.775	584.8375	673.3375	739.3
Improvement in hardness <i>HV</i> , %	0	5.2	14.67	33

## 7.2. Relationship between Coating Thickness and Spray Time

The test carried out for pin and the disc for three types of samples, with different layers of paint, where the first group was of 50, 70 and 80  $\mu\text{m}$  at coating time of 5, 10 and 15 sec, respectively, and the relation between the spray time and coat thickness is shown in Fig. 10.

The micro hardness test of samples carried for 8 samples as indicated in Table 5 and Fig. 11 with coating thickness of 50, 70 and 80  $\mu\text{m}$ . The used load was of 4.905 N during 10 sec.

## 7.3. Microstructure of Coated Samples

The SEM photography done to calculate the thickness of the coating layers for specimens for different coating time of 5, 10, and 15 sec, this test done for several specimens for each coating time and show the thicknesses of 50, 70, and 80  $\mu\text{m}$ , respectively.

## 8. CONCLUSION

The Nano coating by using of spray flame on the surface of cast iron high chromium grinding balls will increased resistance to mechanical wear of the surface by 75% for coat thickness of 70  $\mu\text{m}$ . As the thickness of the nanocoating increases, there is an increase in microhardness reach to 14.6% for the coated samples at a thickness of 70  $\mu\text{m}$  of the nanocoating. The high temperature of the flame used in the coating process to melting part of the surface layer of the base metal at certain points. That leads to increasing the bonding of the metal coating with the base metal. The coating layer

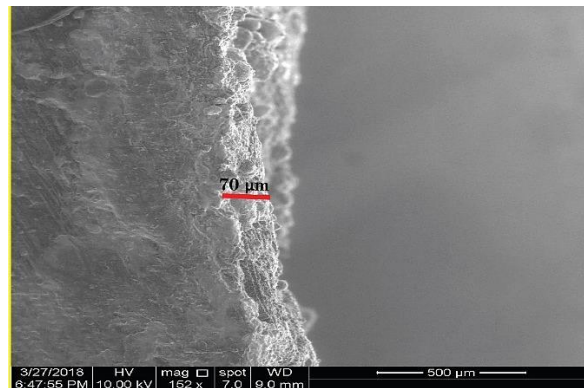


Fig. 12. SEM morphology of layer thickness.

of 80  $\mu\text{m}$  thickness subjected to flaking and debonding after some time so that it is not prefer to use as coating layer.

## ACKNOWLEDGMENT

The authors would like to acknowledge the help offered by Nanotechnology and Advanced Materials Research Unit (NAMRU) and Laboratories of Mechanical Engineering Department at Faculty of Engineering University of Kufa, Iraq. The authors are thankful the mechanical workshops in Kufa cement plant, Iraq.

## REFERENCES

1. J. D. Gates, G. J. Gore, M. J.-P. Hermand, M. J.-P. Guerineau, P. B. Martin, and J. Saad, *Wear*, **263**, Iss. 1–6: 6 (2007); <https://doi.org/10.1016/j.wear.2006.12.033>
2. Xinghai Shao, Jingpei Xie, Wenyan Wang, Yan L, Pingan Zhou, and Huiwu Yu, *Applied Mechanics and Materials*, **217–219**: 2410 (2012); <https://doi.org/10.4028/www.scientific.net/AMM.217-219.2410>
3. Debalina Bhattacharjee, Kamaraj Muthusamy, and Sarathi Ramanujam, *Tribology Transactions*, **57**, Iss. 2: 292(2014); <https://doi.org/10.1080/10402004.2013.870272>
4. O. F. Higuera-Cobos, F. D. Dumitru, and D. H. Mesa-Grajales, *Revista Facultad de Ingeniería*, **25**, Iss. 41: 93 (2016); <http://dx.doi.org/10.1179/030716979803276228>
5. A. Santos, C. Gonzalez, and Z. Y. Ramirez, *Journal of Physics: Conference Series*, **786**: 1 (2017); [doi:10.1088/1742-6596/786/1/012011](https://doi.org/10.1088/1742-6596/786/1/012011)
6. M. S. Powell, N. S. Weerasekara, S. Cole, R. D. LaRoche, and J. Favier, *Minerals Engineering*, **24**: 341 (2011); [doi:10.1016/j.mineng.2010.12.012](https://doi.org/10.1016/j.mineng.2010.12.012)
7. D. Kopyciński, S. Piasny, M. Kawalec, and A. Madizhanova, *Archives of Found Engineering*, **14**, Iss. 1: 63 (2014); [doi.org/10.2478/afe-2014-0015](https://doi.org/10.2478/afe-2014-0015)
8. W. M. Rainforth, *Journal of Materials Science*, **39**, Iss. 22: 6705 (2014); [doi:10.1023/B:JMSE.0000045601.49480.79](https://doi.org/10.1023/B:JMSE.0000045601.49480.79)
9. Cecilio Alvares da Cunha, Nelson Batista de Lima, Jose Roberto Martinelli, Ana Helena de Almeida Bressiani, Armando Guilherme Fernando Padiãl, and Lalgudi Venkataraman Ramanathan, *Materials Research*, **11**, Iss. 2: 137 (2008); [doi.org/10.1590/S1516-14392008000200005](https://doi.org/10.1590/S1516-14392008000200005)
10. Firas Q. Mohmmad, *Studying the Effect of Some Powders Used in Thermal Spraying by Flame One Some of the Mechanical Properties of Medium Carbon Steel* (M.Sc. Thesis in Metallurgy Engineering of University of Technology: 2007).
11. Magdy M. El Rayes, Hany S. Abdo, and Khalil Abdelrazek Khalil, *Int. Electrochemical Sci.*, **8**: 1117 (2013).
12. American Standard of Testing and Material (ASTM), ‘Standard Test Method for Wear Testing with a Pin-on-Disk Apparatus’ (ASTM G99–17: 2017).